International Journal of Engineering & Technology, 7 (2.7) (2018) 114-119

International Journal of Engineering & Technology

Website: www.sciencepubco.com/index.php/IJET

Research Paper



Pattern classification of interstitial lung disease in high resolution clinical datasets: A systematic review

S Ummay Atiya[1]*, N.V.K Ramesh[2],

[1]Research scholar, ECE Dept., KlEF, vaddeswaram, Andhra Pradesh, India
[2]Associate Professor, ECSE Dept., KLEF, vaddeswaram, Andhra Pradesh, India
**Corresponding author E-mail: atiyaece26.rcew@gmail.com*

Abstract

Automated tissues characterization helps to diagnosis the various diseases including Interstitial lung diseases (ILD). The various features and the several classifiers are used in categorize the different layers depend on the pattern presented in the image. The different types of diseases may occur in the lungs and some of the diseases happen to leave the scars. These scars can be found in the High Resolution Computed Tomography (HRCT) and have different pattern. The different diseases cause the different pattern in the images and these is classified using the efficient classifier that helps to diagnosis the diseases. In this paper, review for the many researches regarding to the classification of the different pattern from the Computed Tomography (CT) images is presented. The evaluation of the efficiency of the methods in terms of classifier and database used for the research is made. The Deep Convolution Neural Network (CNN) provides the promising classifier efficiency compared to the other researches for different pattern. In general, there are five types of pattern is classified: Healthy, ground glass, honeycomb, Fibrosis, and emphysema.

Keywords: *Automated tissues characterization; Deep Convolution Neural Network; ground glass; Interstitial lung diseases; High Resolution Computed Tomography;*

1. Introduction

Interstitial lungs disease (ILD) is kind of inflammation happens in the lungs that make severe scaring in lungs tissues. This types of disease will affect the tissues and space around air sacs in lungs [1]. This causes the series of scares in the lungs that can cause difficulty in breathing. This causes the stiffness in lung tissues, which lead to reduce the capacity of the lungs to carry oxygen to the blood [2]. The major cause of ILD are genetic abnormalities, autoimmune disease and exposed to hazard environments and ILD cannot be diagnosed by the process of radiology [3]. The different ILD patter contains the similar clinical manifestation with each other, which are heterogeneous diseases. The diagnosis of the diseases based on the different ILD pattern of radiological data is difficult even for the experienced physician [4]. Then the biopsy process is used to diagnosis the diseases and this has the bad effect in the health, also increases the cost for surgery [5], [6]. The computer aided diagnosis (CAD) method uses the classification for the diagnosis the diseases depend on the pattern of the image.

The use of automated classification system for the identification of scares in the lungs is becoming important diagnosis process in CAD. Many classification method is proposed for the ordering of lung scars in CT [7]. HRTC is the popular tool for diagnosis by using detection and characterizing numerous disorder of lungs [8]. The texture and shape of the diseases presented in lung images is useful for finding the lung diseases that relates to the disease pathology [9]. Several lung diseases classification techniques have been analyzed for disease differentiation [10]. In this paper, the analysis is done on the research present in classification of ILD based on the feature of HRCT. The latest research is considered for the investigation of classifier performance in class of identifying the lung diseases based on the scares of the lungs. The Deep CNN provides the better classification based on the different pattern of the ILD in the HRCT. From the research of M. Ajin and L. Mredhula [31], the several classifiers are used such as ANN, KNN etc., and the Kernel based SVM provides the better result compared to the other classification methods.

2. Research methodology

The method involves of two steps, the first one would extended the limited labels from the dataset to all the pixel in the lung region. The multi-class image segmentation and labelling helps to analysis the all possible way to identify the ILD pattern from the given part of whole lung slice, which is taken manually. The pairwise potentials builds from the fully attached Conditional Random Field (CRF) to the pairs of pixels in the image [11]. The optimization of the CRF is conducted while passing the message that naturally handles the multi-class labelling. The unary energies of the CRF are learned from the CNN-based image patch labelling. The disease part of the images is manually taken from the images by the radiologists are also included in the CRF as hard constraints.

The second phase predicting the multiple labels simultaneously on the same slice and is processed in the database. The two variation of the multi-label deep CNN regression for better performance [12]. First multi-label regression is trained in an end-to-end CNN network, which reduces the loss function in order to calculate the exact pixel present per ILD class. At the second, the feature maps convolutional activation at various network layers are formed spatially and this encode using Fisher Vectors (FV) methods. The

Copyright © 2016 Authors. This is an open access article distributed under the Creative Commons Attribution License, which permits unrestricted use, distribution, and reproduction in any medium, provided the original work is properly cited.

spatial configuration of the convolution activations is removed by this encoding method and turned into representations of location-invariant, this types of CNN is called FV-CNN. The unorderly features are present are trained using multivariate linear regressor to regress the number of ILD pixel [13]. The segmentation is done for the fivefold cross-validation (CV) to identify the general ILD classes of honeycomb, Fibrosis, emphysema and ground glass [14], [15], [16]. The overview of the detection of the ILD from the database is shown in the figure 1 with ROI segmentation and labeling.

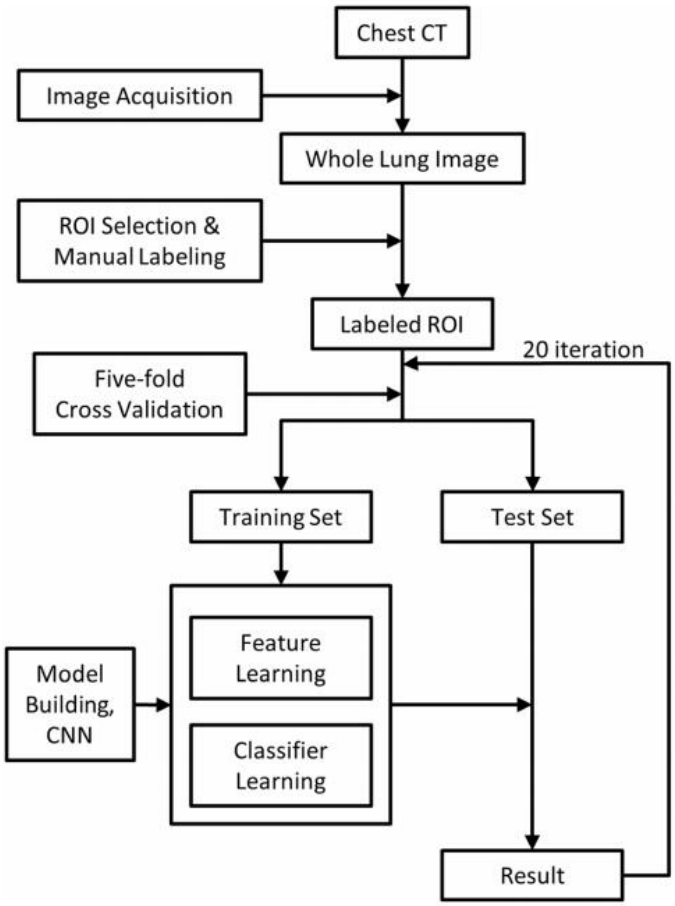


Fig. 1: Overview of the detection of ILD

2.1 Segmentation Label Propagation

The Maximum a posteriori (MAP) interpretation in a CRF is allocated as pixel, which is formulated by the segmentation problem [17]. An effective completely connected with CRF method is consider the account of the long-range image interactions [18], [19]. The conditional distribution from the class labelling X in the image from the database is presented by using CRF method. Let assume as a X random field allocated over the set of variables $\{X_1,...,X_N\}, X_i \in X$ linked with all the pixel $i \in V$ and obtain the label set $L=\{l_1,...,l_k\}$ of label categories. The labelling of X is derived from the images with MAP determination of log-likelihood:

$$E(x)=\sum_i \varphi_u(x_i)+\sum_{i<j}\varphi_p(x_i,x_j) \tag{1}$$

Where i and j values from $1 to N$, $\varphi_u(x_i)$ is unary potential, is calculated separately by using CNN classifier for every pixel/patch. The pairwise potentials in this model have the method.

$$\varphi_p(x_i,x_j)\sum_{m=1}^{k}k(f_i,f_j) \tag{2}$$

$$=u(x_i,x_j)\sum_{m=1}^{k}\omega^{(m)}k^{(m)}(f_i,f_j) \tag{3}$$

Each k^m is a Gaussian kernel

$$k^{(m)}(f_i,f_j)=\exp(-\frac{1}{2}(f_i-f_j)^T\Lambda^{(m)}(f_i-f_j)) \tag{4}$$

Where f_i *and* f_j denoted as the feature vector in an arbitrary feature space of the pixel i *and* j, the compatibility function is given as u and the linear combination weights $\omega^{(m)}$.

The two-kernel potentials are used in this method, denoted in manner of the CT attenuation vectors I_i *and* I_j and their respective positions are p_i *and* p_j:

$$K(f_i,f_j)=\omega^{(1)}\exp\left(-\frac{|p_i-p_j|^2}{2\theta_\alpha^2}-\frac{|I_i-I_j|^2}{2\theta_\beta^2}\right)+\omega^{(2)}\exp\left(-\frac{|p_i-p_j|^2}{2\theta_\gamma^2}\right) \tag{5}$$

From the equation (5), the appearance kernel is given in the first term, which shows the affinity of neighbor pixel with same level of attenuation in the CT and smoothness of the kernel is produced by the second term that removes the small isolated regions. The parameters of $\theta_\alpha,\theta_\beta,\theta_\gamma$ are used to change the closeness and similarity, and the message passing algorithm is used to make the efficient approximation of the interferences of fully connected

random field [20], [21]. The message is passed for every iteration functions, message passing, a local update, and compatibility transform can be implemented applying the Gaussian filtering technique in feature space [22]. In the count of variables N and the count of sublinear edges, the complexity is reduced form quadratic to linear is shown in figure 2.

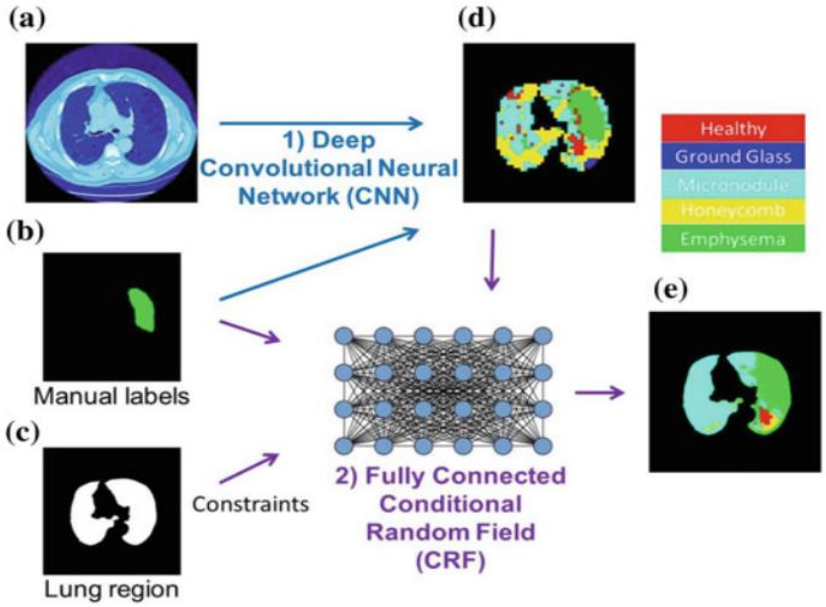


Fig. 2: The segmentation of images by using CNN classifiers and their results. (a) three channel of different HU window with RGB value, (b) Annotated ROI, (c) Annotated lung mask, (d) CNN classifier at the spatial interval of 10 pixels, (e) Final result image.

2.2 Unary classifier using CNN

There are several works are present in the classification of ILD using pattern classification and few researches focuses on image patch based classification using hand-crafted or CNN learned features. The five common patterns classified in the ILD segmentation are fibrosis, ground glass, micronodules, emphysema and healthy tissues as shows in figure 3. The size of the patch images are 32×32 pixels present within the ROI annotations range. The five patterns are extracted from the images and trained into the CNN classifier. The most common CNN AlexNet model utilize the image patch dataset is trained on ImageNet in order to fine-tune. The image patch size is increased from 32×32 to 224×224 and for accommodate the CNN model, three channels are generated with different HU windows.

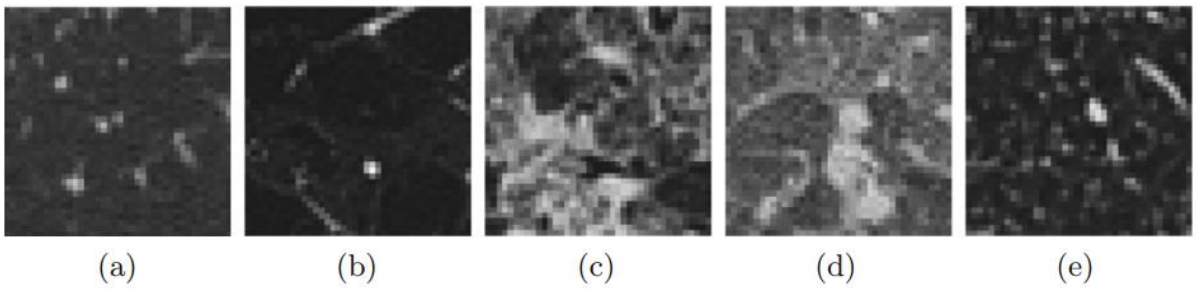


Fig. 3: (a) Healthy, (b) emphysema, (c) Fibrosis, (d) Ground glass, (e) micronodules.

2.3 Hard constraints

The labeling of the images is prepared by the radiologist are stored in the database, which are assigned as ground truth. The hard-reset are applied in the hard constrained regions of the images for each CRF iteration of message passing, due to it has to reliable with their ground truth label. In this type of cases, the message passing only happens in the pixel of unlabeled lung image made out from the regions of hard constrained and c the lung field only taken for the labelling. This is independent of the condition of pattern on image present outside of the lung mask. From the equation (5), the parameters $\theta_\alpha, \theta_\beta, \theta_\gamma$ are taken as the small constant as the value of 0.001 for linking lung of any pixel and (p_i, p_j) non-lung spatial indexes. So the related $k(f_i, f_j)$ has a disappearing value, which is equal to the null message passing.

The possible ways are explored for the ILD labels propagate to the whole lung slice from limited drawn regions in pixel wise multiclass image segmentation and labeling. The pairwise potentials are construct on every pairs of pixel from the image based on the fully connected CRF. The optimization is carried out in the CRF by using message passing, which is capable of handling the multiclass labeling and the unary energies are learned based on the CNN using image patch labeling. The ground truth is combined as hard constraints in the CRF and there are many databases are available for the classification of ILD and the segmented results are evaluated with help of expert radiologist.

2.4 Multi-label ILD regression

The two major components are used in the algorithm, (1) To calculate the area of the ILD using deep CNN regression of multi-label technique by observation or provide the binary status of

"non- appearing" and "appearing" from a squared L2 loss function and these are utilized to solve the convolution property of ILDs. (2) The extraction of the activation layers from the different depth of the CNN network and the method of multivariate linear regression used to discriminate the spatially unordered Fisher vector features.

2.5 CNN architecture

Deep CNN is used to measure the spatial present in ILD images, where many pathology patterns is co-exist. Instead of highly utilize the logistic-regression loss or softmax [23] for CNN-based classification, the squared L2 loss function is used [24], [25], [26] and there are many number of methods are available for regression label in the image. There is one direct method is present to measure the total count of pixel of ILD pattern per disease to represents its level of disease [27]. The step function is used to characterize the existence or absence of diseases, where the value for stage threshold is set from the knowledge of the clinical use. The label is assigned as one if the count of pixel in the ILD image is larger than the T, otherwise zero. A more complex model contains function of the piecewise linear transform and the pixel number is calculated towards the range (0, 1).

If there are N number of images are available and type c of ILD patterns is identified, the label vector of the i^{th} image is characterized as a c-length multivariate vector $y_i = [y_{i1}, y_{i2}, ..., y_{ic}]$. The healthy portion of the lungs or there is no pattern present in the regions are denoted in the all-zero labelling vector depend on the ground truth pattern to the ILD image. The L2 cost function to be reduced, is defined as:

$$L(y_i, \hat{y}_l) = \sum_{i=1}^{N} \sum_{k=1}^{c} (y_{ik} - \hat{y}_{ik})^2 \quad (7)$$

There are various successful CNN are present like as AlexNet and VGGNet. CNN-F is employed for the performance and efficiency depend on the availability of database, creates a variation of AlexNet. The five convolution layers is presented in CNN-F, that is tracked by two layers that are completely connected (FC) [28]. The squared L2 loss function is set for the last layer and four classes of ILD and the health tissues are investigated in some experiments and four ILD tissues: Fibrosis, honeycomb, ground glass and emphysema. The length of y_i is c=4 to express these classes of four ILD [29]. The CNN parameter has randomly initialized works better than the models of pre-trained ImageNet and stochastic gradient descent optimize the model parameters [30].

2.6 Unorder pooling regression via Fisher Vector Encoding

Testing a CNN feature activation encoding spatially invariant is used in along with CNN based regression. The outcome of every k-th layer is treated in the descriptor field $X_k \in \mathbb{R}^{W_k \times H_k \times D_k}$ as 3D convolutional layer, where width and height of the fields are denoted as $W_k, H_k \text{ and } D_k$ is the count of features channels. The complete activation map of deep feature is given as feature vectors $W_k \times H_k$ and all the feature vectors is the dimension of D_k.

The FV encoding is invoke to eliminate of vectors $W_k \times H_k$ with the spatial configurations present in an activation map and soft quantized is done for each descriptor $x_i \in X_k$ help of mixture model of Gaussian. The differences of first-order and second-order $(u_{i,m}^T, v_{i,m}^T)$ between any X_i descriptor and each of the vectors $\{\mu_m\}, m = 1, 2, ..., M$ of the Gaussian cluster means are gathered in a 2M D_k -dimensional image representation:

$$f_i^{FV} = [u_{i,1}^T, v_{i,1}^T, ..., u_{i,m}^T, v_{i,M}^T]^T \quad (6)$$

The results of the FV feature encoding in high 2M D_k dimensionally for the deep features of X_k. Principal component Analysis (PCA) is used to computational and memory efficiency and also to reduce features f_i^{FV} to a lower-dimensional parameter space. The presence and absences of ILDs is identify by using the multivariate linear regression y_i label vectors of ground truth and with the image features of PCA present in the low-dimensional value.

3. Comparison table

The lung diseases cause the different patterns of scars in the lungs and different patterns of scars may present in the lungs. The analysis the scars patterns helps to identify the lung disease and these kind of scars has been found in the HRCT images. The latest researches of the HRCT lung pattern classifiers are consider in this paper.

Author and Publication	Classifier Employed	Dataset	Advantage	Limitation	Performance Analysis
M. Ajin and L. Mredhula, [31]	ANN, KNN, Deep CNN Hybrid Kernel based SVM.	Lung Image database Consortium	This method helps to analysis the various methods using the feature extraction, selecting feature, classification and also shows that Hybrid Kernel based SVM shows the better performance.	This method is done with the approximately equal number of image patches for training and testing sets, if the training is set low and testing is set high then the accuracy is reduced.	ANN = 57.50 %, KNN = 72.94 %, Deep CNN 84.14 %, Hybrid Kernel based SVM = 90.52 %.
R. Joyseeree, et al. [32].	Radial basic function based SVM.	ILD database	The proposed system provide the better accuracy than the state-of-art method due to different patch selection and evaluation method.	The misclassification of the pattern occurs in the annotated area and causes to reduce in accuracy.	Multicast tissue classification accuracy = 80.31 %.
H. M. Nurmi, et al. [33]	Independently reclassified by idiopathic interstitial pneumonia	Kuopio University Hospital database	This shows the correlation relation between the reticulation, traction bronchiectasis and architectural distortion to the decrease survival.	This method is only applied to the little dataset.	Hazard ration, GGO = 1.079, Reticulation = 1.144.
J. Lim, et al [34]	context-sensitive support vector machine (csSVM)	In this research, radiologist categorized 84 whole lung images are used as the database.	This technique can be utilized for the multi-class classification problem and the CRF cannot address this problem.	This method is applied to the 2D images only and 3D images provides the much more data about the diseases.	Accuracy for whole lungs, CsSVM = 60.30±13.95, Time (s) = 3.05±0.91.

S. Jun , et al. [35]	ensemble classifiers	Siemens datasets	The ensemble classifiers uses the individual classifier to increases the performance of the classification in analyses, bagging and stacking has high performance than the individual classifiers.	This technique is not applied to the 3D volumetric images, which provides the more information about diseases.	SVM = 0.62, NB = 0.54, RF = 0.58.
S.H. Jun1, et al. [36]	SVM classifier	Stimulated dataset	The result is compared with the existing method and this provides the better result, also helps for supporting decision for clinical.	This methods categorized into two diseases.	Average accuracy = 81 %.
A.O. Neil, et al. [39]	CNN	MedGift dataset	This has better result for even the low-level problem such as texture classifier, well defined deep learning architectural with sufficient capacity.	This performance is made only for the little amount of dataset.	Accuracy = 79%,
A. Depeursing, et al. [40]	blockwise classification	rich Internet application	The developed system enables the objective and customizable in textbook and personnel collections.	The implementation of clinical workflow with CBIR based CAD is complex on both user's side and an algorithm side.	Accuracy, Healthy tissues = 87.94 %, Emphysema = 96.3 %, Fibrosis = 89.02 %.
J.W. Moon, et al. [42]	SVM classifier based on LIBSVM library3	The database is taken from the Institutional Review Board of Samsung Medical Center	This method provides high accuracy compared to the probabilistic atlas-based method.	This method has to be evolved from the larger dataset.	Accuracy, 2D features = 88.32 %, 3D features = 90.47 %.
A. Depeursinge, et al. [40]	Multilayer perceptron, k-nearest neighbour, naive Bayes, J48 decision trees, and SVM.	The dataset was taken from the Talisman project at Geneva University Hospitals and University of Geneva	SVM has better tradeoff between error rate and classify the better than other classifiers.	The implementation is not made in 3D images.	Accuracy, SVM = 0.8907, Naive Bayes = 0.3778, J48 = 0.7555

The deep neural technique provides the better classification result for the pattern recognition and despite this fact, it still has some complex set that was challenging for the convolution neural network. Those tasks requires the explicit memory for store the facts needed for classification of pattern. So, the classifier such as Neural turning machines, Memory based neural networks etc., has the possibility to have the classification accuracy as ±2% than the state-of-art method for classification of ILD.

4. Conclusion

ILD is a method to diagnosis the group of lung disease affecting the tissues, it may lead to the severe disease in case if it is not properly diagnosed. These kinds of diseases have the similar clinical manifestation with each other making it difficult for diagnosis the diseases even by the experienced physicians. Many research is processed in the classification of the diseases from the pattern present in the datasets taken from the CT. In this paper, the analysis of the different research for the sorting of the ILD in the CT images. Usually, there are five patterns are classified: honeycombing, consolidation, micronodules, reticulation, Ground glass opacity and healthy tissues. The deep CNN and kernel based SVM provides the better classification result compared to the other classifiers. The different research is studied and compared in the comparison table, which also has the advantages and disadvantageous of their method. There are lot of databases are available for the ILD and some of them are available freely. In the research of Moon, *et al* [42], SVM is used as the classifier and provide the accuracy up to 88.32%.

Acknowledgement

This is a text of acknowledgements. Do not forget people who have assisted you on your work. Do not exaggerate with thanks. If your work has been paid by a Grant, mention the Grant name and number here.

References

[1] Korfiatis PD, Kalogeropoulou C, Karahaliou AN, Kazantzi AD & Costaridou LI, "Vessel tree segmentation in presence of interstitial lung disease in MDCT", *IEEE Transactions on Information Technology in Biomedicine*, Vol. 15, No. 2, pp. 214-220, 2011.

[2] Okumura E, Kawashita I & Ishida T, "Computerized Classification of Pneumoconiosis on Digital Chest Radiography Artificial Neural Network with Three Stages", *Journal of digital imaging*, Vol. 30, No. 4, pp. 413-426, 2017.

[3] Depeursinge A, Pad P, Chin AS, Leung AN, Rubin DL, Müller H & Unser M, "Optimized steerable wavelets for texture analysis of lung tissue in 3-D CT: Classification of usual interstitial pneumonia", *Proceedings of the 12th International Symposium on In Biomedical Imaging (ISBI)*, pp. 403-406, 2015.

[4] Dash JK, Mukhopadhyay, S, Garg MK, Prabhakar N & Khandelwal N, "Multi-classifier framework for lung tissue classification", *Proceedings of the Students' Technology Symposium (TechSym)*, pp. 264-269, 2014.

[5] Depeursinge A, Van de Ville D, Platon A, Geissbuhler A, Poletti PA and Muller H, "Near-affine-invariant texture learning for lung tissue analysis using isotropic wavelet frames", *IEEE Transactions on Information Technology in Biomedicine*, Vol. 16, No. 4, pp.665-675, 2012.

[6] Song Y, Cai W, Zhou Y & Feng DD, "Feature-based image patch approximation for lung tissue classification", *IEEE transactions on medical imaging*, Vol. 32, No. 4, pp. 797-808, 2013.

[7] Kockelkorn TT, Sánchez CI, Grutters JC, Ramos R, de Jong PA, Viergever MA, Ramos J, Schaefer-Prokop C & van Ginneken B, "Interactive classification of lung tissue in CT scans by combining prior and interactively obtained training data: A simulation study", *Proceedings of the 21st International Conference on Pattern Recognition (ICPR)*, pp. 105-108, 2012.

[8] Depeursinge A, Vargas A, Platon A, Geissbuhler A, Poletti PA & Müller H, "3D case–based retrieval for interstitial lung diseases", *Proceedings of the MICCAI International Workshop on*

Medical Content-Based Retrieval for Clinical Decision Support, pp. 39-48, 2009.

[9] Vogl WD, Prosch H, Müller-Mang C, Schmidt-Erfurth U & Langs G, "Longitudinal alignment of disease progression in fibrosing interstitial lung disease", *Proceedings of the International Conference on Medical Image Computing and Computer-Assisted Intervention*, pp. 97-104, 2014.

[10] Fetita C, Chang-Chien KC, Brillet PY, Prêteux F & Grenier P, "Diffuse parenchymal lung diseases: 3D automated detection in MDCT", *Proceedings of the International Conference on Medical Image Computing and Computer-Assisted Intervention*, pp. 825-833, 2007.

[11] Vo KT & Sowmya A, "Directional multi-scale modeling of high-resolution computed tomography (hrct) lung images for diffuse lung disease classification", *Proceedings of the International Conference on Computer Analysis of Images and Patterns*, pp. 663-671, 2009.

[12] Gupta RD, Dash JK & Mukhopadhyay S, "Content based retrieval of interstitial lung disease patterns using spatial distribution of intensity, gradient magnitude and gradient direction", *Proceedings of the International Conference on Systems in Medicine and Biology (ICSMB)*, pp. 58-61, 2016.

[13] Hamzah MFM, Kasim RM, Yunus A, Rijal OM & Noor NM, "Detection of Interstitial Lung Disease using correlation and regression methods on texture measure. *Proceedings of the IEEE International Conference on Imaging, Vision & Pattern Recognition (icIVPR)*, pp. 1-4, 2017.

[14] Raj MD & Sulochana CH, "An efficient lung segmentation approach for interstitial lung disease", *Proceedings of the International Conference on Circuit, Power and Computing Technologies (ICCPCT)*, pp. 1211-1216, 2014.

[15] Ebrahimian H, Noor NM, Rijal OM, Yunus A & Kassim RM, "Gabor texture measure in interstitial lung disease discrimination using high resolution computed tomography thorax images", *Proceedings of the IEEE Conference on Biomedical Engineering and Sciences (IECBES)*, pp. 827-831, 2014.

[16] Ming JTC, Noor NM, Rijal OM, Kassim RM and Yunus A, "Enhanced automatic lung segmentation using graph cut for Interstitial Lung Disease", *Proceedings of the IEEE Conference on Biomedical Engineering and Sciences (IECBES)*, pp. 17-21, 2014.

[17] Vo KT and Sowmya A, "Scale-space representation of lung HRCT images for diffuse lung disease classification. *Proceedings of the International Conference on Image and Signal Processing*, pp. 550-558, 2010.

[18] Yokota K, Maeda S, Kim H, Tan JK, Ishikawa S, Tachibana R, Hirano Y & Kido S, "Automatic detection of GGO regions on CT images in LIDC dataset based on statistical features. In Soft Computing and Intelligent Systems (SCIS)", *Proceedings of the Joint 7th International Conference on and Advanced Intelligent Systems (ISIS)*, pp. 1374-1377, 2014.

[19] Shouno H, Suzuki S & Kido S, "A transfer learning method with deep convolutional neural network for diffuse lung disease classification", *Proceedings of the International Conference on Neural Information Processing*, pp. 199-207, 2015.

[20] Ramos J, Kockelkorn TT, Ramos I, Ramos R, Grutters J, Viergever MA, van Ginneken B and Campilho A, "Content-based image retrieval by metric learning from radiology reports: Application to interstitial lung diseases", *IEEE journal of biomedical and health informatics*, Vol. 20, No. 1, pp.281-292, 2016.

[21] Anthimopoulos M, Christodoulidis, S, Christe A & Mougiakakou S, "Classification of interstitial lung disease patterns using local DCT features and random forest", *Proceedings of the 36th Annual International Conference on Engineering in Medicine and Biology Society (EMBC)*, pp. 6040-6043, 2014.

[22] Noor NM, Rosid R., Azmi MH, Rijal OM, Kassim RM & Yunus A, "Comparing watershed and FCM segmentation in detecting reticular pattern for interstitial lung disease", *Proceedings of the IEEE EMBS Conference on Biomedical Engineering and Sciences (IECBES)*, pp. 944-949, 2012.

[23] Anthimopoulos M, Christodoulidis S, Ebner L, Christe A and Mougiakakou S, "Lung pattern classification for interstitial lung diseases using a deep convolutional neural network", *IEEE transactions on medical imaging*, 35(5), pp.1207-1216, 2016.

[24] Wei Y, Xia W, Lin M, Huang J, Ni B, Dong J, Zhao Y & Yan S, "Hcp: A flexible cnn framework for multi-label image classification", *IEEE transactions on pattern analysis and machine intelligence*, Vol.38, No. 9, pp.1901-1907, 2016.

[25] Gao M, Bagci U, Lu L, Wu A, Buty M, Shin HC, Roth H, Papadakis GZ, Depeursinge A, Summers RM & Xu Z, "Holistic classification of CT attenuation patterns for interstitial lung diseases via deep convolutional neural networks", *Computer Methods in Biomechanics and Biomedical Engineering: Imaging & Visualization*, pp.1-6, 2016.

[26] Krizhevsky A, Sutskever I & Hinton GE, "Imagenet classification with deep convolutional neural networks", *Proceedings of the Advances in neural information processing systems*, pp. 1097-1105, 2012.

[27] Kaur S, Hooda R, Mittal A & Sofat S, "Deep CNN-Based Method for Segmenting Lung Fields in Digital Chest Radiographs", *Proceedings of the Advanced Informatics for Computing Research*, pp. 185-194, 2017.

[28] Wang Q, Zheng Y, Yang G, Jin W, Chen X & Yin Y, "Multiscale Rotation-Invariant Convolutional Neural Networks for Lung Texture Classification", *IEEE journal of biomedical and health informatics*, Vol. 22, No. 1, pp.184-195, 2018.

[29] Christodoulidis S, Anthimopoulos M, Ebner L, Christe A & Mougiakakou S, "Multisource transfer learning with convolutional neural networks for lung pattern analysis", *IEEE journal of biomedical and health informatics*, Vol. 21, No. 1, pp.76-84, 2017.

[30] Kim GB, Jung KH, Lee Y, Kim HJ, Kim N, Jun S, Seo JB & Lynch DA, "Comparison of Shallow and Deep Learning Methods on Classifying the Regional Pattern of Diffuse Lung Disease", *Journal of digital imaging*, pp.1-10, 2017.

[31] Ajin M & Mredhula L, "Diagnosis of Interstitial Lung Disease by Pattern Classification", *Procedia Computer Science*, Vol. 115, pp.195-208, 2017.

[32] Joyseeree R, Müller H & Depeursinge A, "Rotation-Covariant Tissue Analysis for Interstitial Lung Diseases Using Learned Steerable Filters: Performance Evaluation and Relevance for Diagnostic Aid", *Computerized Medical Imaging and Graphics*, 2018.

[33] Nurmi HM, Kettunen HP, Suoranta SK, Purokivi MK, Kärkkäinen MS, Selander TA & Kaarteenaho RL, "Several high-resolution computed tomography findings associate with survival and clinical features in rheumatoid arthritis-associated interstitial lung disease", *Respiratory Medicine*, Vol. 134, pp.24-30, 2018.

[34] Lim J, Kim N, Seo JB, Lee YK, Lee Y & Kang SH, "Regional context-sensitive support vector machine classifier to improve automated identification of regional patterns of diffuse interstitial lung disease", *Journal of digital imaging*, Vol. 24, No. 6, pp. 1133-1140, 2011.

[35] Jun S, Kim N, Seo JB, Lee YK & Lynch DA, "An Ensemble Method for Classifying Regional Disease Patterns of Diffuse Interstitial Lung Disease Using HRCT Images from Different Vendors", *Journal of digital imaging*, Vol. 30, No. 6, pp. 761-771, 2017.

[36] Jun S, Park B, Seo JB, Lee S & Kim N, "Development of a Computer-Aided Differential Diagnosis System to Distinguish Between Usual Interstitial Pneumonia and Non-specific Interstitial Pneumonia Using Texture-and Shape-Based Hierarchical Classifiers on HRCT Images", *Journal of digital imaging*, pp.1-10, 2017.

[37] O'Neil A, Shepherd M, Beveridge E & Goatman K, "A Comparison of Texture Features Versus Deep Learning for Image Classification in Interstitial Lung Disease", *Proceedings of the Annual Conference on Medical Image Understanding and Analysis*, pp. 743-753, 2017.

[38] Depeursinge A, Vargas A, Gaillard F, Platon A, Geissbuhler A, Poletti PA & Müller H, "Case-based lung image categorization and retrieval for interstitial lung diseases: clinical workflows", *International journal of computer assisted radiology and surgery*, Vol. 7, No. 1, pp.97-110, 2012.

[39] Moon JW, Bae JP, Lee HY, Kim N, Chung MP, Park HY, Chang Y, Seo JB & Lee KS, "Perfusion-and pattern-based quantitative CT indexes using contrast-enhanced dual-energy computed tomography in diffuse interstitial lung disease: relationships with physiologic impairment and prediction of prognosis", *European radiology*, Vol. 26, No. 5, pp.1368-1377, 2016.

[40] Depeursinge A, Iavindrasana J, Hidki A, Cohen G, Geissbuhler A, Platon A, Poletti PA & Müller H, "Comparative performance analysis of state-of-the-art classification algorithms applied to lung tissue categorization", *Journal of digital imaging*, Vol. 23, No. 1, pp.18-30, 2010.